COMPARISON OF F_2-BASED GASES FOR HIGH-RATE DRY ETCHING OF Si

D. C. Hays, K. B. Jung, Y. B. Hahn*, E. S. Lambers, and S. J. Pearton
Dept. of Materials Science and Engineering, University of Florida, Gainesville, FL 32611

J. Donahue and D. Johnson
Plasma Therm, St. Petersburg, FL 33716

R. J. Shul
Sandia National Laboratories, Albuquerque, NM 87185

ABSTRACT

Four different F_2-based gases (SF_6, NF_3, PF_5, and BF_3) were examined for high rate Inductively Coupled Plasma etching of Si. Etch rates up to ~8μm/min were achieved with pure SF_6 discharges at high source power (1500W) and pressure (35mTorr). A direct comparison of the four feedstock gases under the same plasma conditions showed the Si etch rate to increase in the order $BF_3 < NF_3 < PF_5 < SF_6$. This is in good correlation with the average bond energies of the gases, except for NF_3, which is the least strongly bound. Optical emission spectroscopy showed that the ICP source efficiently dissociated NF_3, but the etched Si surface morphologies were significantly worse with this gas than with the other 3 gases.

* Permanent address: Dept of Chemical Engineering, Chonbuk National University, Chonbuk National University, Chonju 561-756, Korea.

DISCLAIMER

INTRODUCTION

There is currently tremendous interest in the development and technological exploitation of microsensors fabricated in part by micromachining of Si[1-6]. The applications include accelerometers, gyroscopes, pressure sensors, drug delivery systems, chemical sensors, programmable diffraction gratings, and micromotors[7]. Most Si etching for Micro Electro-Mechanical Systems (MEMS) is performed with crystallographic KOH-based solutions[2]. However, there are significant advantages to the use of dry etching for improved process flexibility and compatibility with standard Si microelectronics fabrication[1]. Disadvantages with KOH wet etching include the difficulty of etching to known depths, unavailability of submicron etching precision, variance in etching properties of Si wafers from different vendors, loading effects and fluid distribution effects in etch baths. Dry etching can remedy these problems.

Currently there are two approaches to the dry etching for Si MEMS, both of which are able to prevent undercutting of the feature sidewalls:

(i) cryogenic SF_6-based plasma etching, in which the sample is held at a low temperature[8-14]. This temperature is sufficiently low that the SiF_x etch products are no longer volatile unless they are desorbed by ion-assistance. Since the ions only strike the horizontal surfaces and not the feature sidewalls, undercutting is suppressed. The drawback of this method is its complexity and low throughput because of the wafer cooling requirements.

(ii) the so-called Bosch process[15], in which the feature sidewalls are continually covered by polymer deposition during a sequential etch/deposition

process involving alternating SF_6/C_4F_8 plasmas. The drawback of this method is its relatively low average etch rate (~ 4-5μm/min).

It would appear that a comparative study of F_2-based feedstock gases for high-rate Si etching would be useful in determining whether SF_6 is the optimum choice in (ii) above. The absolute reaction rate of F atoms with single crystal Si follows[16].

$$\text{Rate (Å/min)} = 2.9\times10^{12} T^{1/2} \exp\left(-E_F/RT\right)$$

where T is the absolute substrate temperature, N_F the F-atom number density, R the gas constant, and E_F the measured activation energy of 2.5 kcal/mol. From this equation it is clear that one must increase the fluorine atomic neutral density in order to increase the Si etch rate. It is not practical to increase the substrate temperature because of the need to use photoresist or polymer masking materials with low thermal stabilities. Similarly, the reaction rate could be enhanced by providing a substantial energetic ion flux to the Si surface. The ion energy, however, must be kept low under these conditions to avoid mask degradation and loss of etch selectivity. Alternative plasma chemistries including Cl or Br containing plasmas are not advantageous since the reaction rates of Cl and Br atoms with Si are slower than with F[17,18].

In this paper we report a study of four different F_2-based feedstock gases (SF_6, NF_3, PF_5, and BF_3) for achieving high-rate Si etching. An Inductively Coupled Plasma (ICP) source is found to readily dissociate these gases, providing a flux of reactive fluorine neutrals for etching of the Si. There are strong differences in the maximum etch rates with the different gas chemistries.

EXPERIMENTAL

The Si samples employed in these experiments were ¼ of 4 inch diameter, (100), B-doped (1Ω•cm) wafers. For etch rate determination a small section of each sample was masked with Apiezon wax, and the step height measured by stylus profilometry after the removal of the mask in acetone. Etching was performed in a Plasma Therm 790 series reactor. This consists of a 3-turn ICP source (2MHz, 1500W), a He backside-cooled, rf-biased (13.56MHz, 0-450W) sample chuck, and radial gas injection into the source through electronic mass flow controllers. In each case the gas load was left constant at 100 standard cubic centimeters per minute (sccm). Preliminary experiments showed the Si etch rates increased with pressure – for most of the work reported here the pressure was maintained at 35mTorr. This is the highest value at which plasma tuning was stable.

The etched surface morphology was examined by both Scanning Electron Microscopy (SEM) and Atomic Force Microscopy (AFM), while the near surface atomic composition was measured by Auger Electron Spectroscopy (AES). The dissociation of the feedstock gases in the ICP source was monitored by Optical Emission Spectroscopy (OES).

RESULTS AND DISCUSSION

Figure 1 (top) shows the effect of ICP source power on Si etch rate for fixed process pressure (35mTorr) and without additional biasing of the sample chuck. In this case the ion energy is approximately equal to the plasma potential (roughly –25eV in this tool at these conditions as determined by Langmuir probe measurements). Since real

micro-machining processes involve long exposures of the mask material to the plasma, it is necessary to minimize the ion energy to prevent erosion of the mask. There are significant differences in the Si etch rates achieved with the four different plasma chemistries, with SF_6 providing for the fastest etch rates. It is instructive to compare the observed etch rate trends with the average bond energies for the gases, shown in Table 1. Note that there is a good correlation between weaker bond energy (i.e. easier dissociation to provide reactive fluorine neutrals) and higher etch rate, except for the case of NF_3. This gas should provide the highest etch rate, based on the assumption of a simple gas dissociation analysis of the process. The etch yields (defined as the number of Si atoms removed per incident ion) were calculated from a simple semi-empirical model that uses extrapolations of ion flux data obtained from Langmuir probe measurements. In SF_6 and PF_5 there is clearly a strong chemical component to the etching, with etch yields in the range 6-10.

The same experiments were repeated with 5W rf chuck bias, which corresponds to dc self-biases of –15 to –30V. The average energy of incident ions is then the sum of this bias and the plasma potential mentioned earlier. The same basic trends in etch rate with ICP power were observed (Figure 2, top), and consequently in the etch yields (Figure 2, bottom).

OES was used to examine emission from the various discharges during etching of Si. Figure 3 shows the spectra from BF_3 and PF_5 processes. In both cases there are clear signatures of the atomic fluorine lines between 680-800nm, and SiF_x etch products (around 450nm). The surprising result is shown in the OES spectra for SF_6 and NF_3 in Figure 4. The SF_6 also produces strong emission from atomic fluorine and the SiF_x etch

products, while the NF_3 spectrum has the strongest F^0 emission intensity of all the gases, as expected from its average bond energy. However, consistent with the etch rate data, we observed only a tiny peak due to the SiF_x etch products.

SEM micrographs of the Si surfaces after 2 min etches in the four different plasma chemistries are shown in Figure 5. The surfaces after PF_5 or BF_3 etching are featureless at this magnification (x1000), while the SF_6-etched surface shows the presence of small pits. We should point out that the human eye does not detect any morphology on this surface and it appears mirror-like. We assume that the high chemical component involved in the SF_6 etching leads to delineation of crystal defects, which etch slightly faster than perfect Si. Note that this is the surface morphology after etching ~16μm with the SF_6 discharge. By sharp contrast, the NF_3-etched surfaces appear cloudy to the eye, and the SEM reveals the presence of shallow pits and linear defects. This is the surface morphology after etching ~1.5μm with the NF_3 discharge.

A more quantitative measure of surface is obtained from the AFM data. Figure 6 shows the Si surfaces before and after etching in the four different plasma chemistries. While the PF_5 and BF_3 produce little change in root-mean-square (RMS) roughness of the Si surface, there is significant roughening with the other two chemistries. As seen in the microstructure, this is due to the delineation of shallow pits in the case of SF_6, whereas for the NF_3 the surface is clearly much rougher on a micro-scale. The RMS values for the etched surfaces are shown in Figure 7 as a function of ICP source power for the four plasma chemistries. Note that the roughness of surfaces etched in SF_6 increases much more rapidly with source power than does etch rate (compare with

Figure 1). This indicates that the etch pits become more obvious above a certain source power, i.e. above certain F^0 densities.

The surprising result in all of these experiments is that NF_3 does not produce the fastest etch rates. One cause might be the formation of a heavily fluorinated (or nitrided) surface layer that prevents reaction of adsorbed fluorine neutrals to form the volatile etch products. We examined the etched surfaces with AES, and surface scans of the SF_6 and NF_3 processed samples are shown in Figure 8. In both cases they look similar to the etched control sample. However, we did notice a small F-residue signal present on the NF_3-etched sample during the first few passes of the scan. These residues were desorbed by the electron probe beam during the analysis, but do not appear in the scan of Figure 8 because that represents the average of 10 consecutive passes of the beam (a standard method when presenting AES data). Note that we did not observe any N-related residues on the NF_3-etched surfaces.

If indeed some type of selvedge layer is the cause of the lower-than-expected Si etch rates in NF_3 discharges, we might expect that a reduction in the F^0 neutral flux might actually enhance the etch rate. The neutral flux can be altered by changing either the process pressure or ICP source power, while an increase in dc self-bias would provide more efficient sputter-desorption of adsorbed reactants and etch products. Figure 9 shows the Si etch rate in NF_3 discharges as a function of each of these parameters. Note that under no set of conditions do we achieve etch rates approaching those obtained with SF_6 (or PF_5). One clear effect of increasing ion energy through higher rf chuck power was a transition from rough morphology to smooth surfaces on NF_3-etched samples, as shown in the AFM data of Figure 10. This would be expected through an enhanced physical

contribution to the etch mechanism, with the angular dependence of ion milling producing faster etching of sharp surface features.

SUMMARY AND CONCLUSIONS

Four different F_2-based plasma chemistries have been compared for the goal of achieving high etch rates for Si. The fastest Si etch rate was obtained in SF_6, with peak rates of ~8μm/min. The simple picture of the Si etch rate being limited by the supply of reactive fluorine neutrals would favor the choice of NF_3. However, experimentally it is observed that NF_3 discharges produce relatively slow Si etch rates, even though the gas is efficiently dissociated in the ICP source. The cause of these low rates is not clear. We have previously observed that SiC is etched more rapidly in NF_3 than in SF_6 discharges. It will probably be necessary to employ some form of in-situ analysis of the NF_3-etched surfaces in order to firmly establish the reason why the etch rates are not higher than observed.

ACKNOWLEDGMENTS

The work at UF is partially supported by a DOD MURI monitored by AFOSR (H.C. DeLong), contract no. F49620-96-1-0026. Sandia is a multiprogram laboratory operated by Sandia Corporation, a Lockheed-Martin company, for the U.S. Dept. of Energy under contract DE-AC-04-94AL85000.

REFERENCES

1. A. A. Ayon, R. A. Braff, C. C. Lin, H. H. Sawin, and M. A. Schmidt, J. Electrochem. Soc., 146, 139 (1999).
2. R. J. Shul, C. G. Willison, and L. Zhang, SPIE, 3511, 252 (1998).
3. R. J. Shul, C. G. Wilson, C. T. Sullivan, S. H. Kravitz, and T. E. Zipperian, Electrochemical Society Proceedings, Vol. 98-2, 564 (1998).
4. C. Seung-Bok Lee, S. Han, N. C. Macdonald, Solid State Sensor and Actuator Workshop, 45 (June, 1998).
5. P. A. Clerc, L. Dellman, F. Gretillat, M. A. Gretillat, P. F. Indermuhle, S. Jeanneret. Ph. Luginbuhl, C. Marxer, T. L. Pfeffer, G. A. Racine, S. Roth, U. Staufer, C. Stebler, P. Thiegaud, and N. F. de Rooij, J. Micromech. Microeng., 8, 272 (1998).
6. W. D. Lang, Mat. Sci. Eng. R., 17, 1 (1997).
7. See for example http://www.mdl.sandia.gov/sensors which gives an overview of microsensor R&D at Sandia National Laboratories.
8. H. Jansen, H. Gardeniers, M. de Boer, M. Elwenspoek, and J. Fluitman, J. Micromech. Microeng., 6, 14-28 (1996).
9. C. P. D'Emic, K. K. Chan, and J. Blum J. Vac. Sci. Technol., B10, 1105 (1992).
10. M. Francou, J. S. Danel, and L. Peccoud, Sensors and Actuators A, 46-47, 17 (1995).
11. C. Linder, T. Tschan, and N. F. de Rooij, Tranducers, 91, 524 (1991).
12. G. S. Oehrlein and Y. Kurogi, Mat. Sci. Eng. R., 24, 153 (1998).
13. S. Tachi, K. Tsujimoto, and S. Odukaira, Appl. Phys. Lett., 52, 616 (1988).
14. S. Tachi, K. Tsujimoto, S. Arai, and T. Kure, J. Vac. Sci. Technol., A9, 796 (1991).

15. Robert Bosch GmbH, patents 4,855,017 and 4,784,720 (USA) and 4241045C1 (Germany).

16. J. W. Coburn and E. Kay, IBM J. Res. Dev., 23, 33 (1979).

17. Z. H. Walker and E. A. Ogryzlo, J. Appl. Phys., 69, 548 (1991).

18. Z. H. Walker and E. A. Ogryzlo, J. Appl. Phys., 69, 2635 (1991).

19. E. L. Muetterties, The chemistry of boron and its compounds, Wiley and Sons, New York, 1967.

20. D. E. C. Cornbridge, Phosphorous: An outline of its chemistry, biochemistry, and technology, Elsevier, New York, 1978.

21. H. J. Emelius, The chemistry of fluorine and its compounds, Academic Press, New York, 1969.

22. M. Stacey, J. C. Tatlow, and A. G. Sharpe, Advances in fluorine chemistry, Vol. 3, Butterworths, Washington, D. C., 1961.

FIGURE CAPTIONS

Figure 1. Si etch rate (top) and etch yield (bottom) as a function of ICP source power in pure SF_6, NF_3, PF_5, or BF_3 discharges (35mTorr, 0W rf chuck power).

Figure 2. Si etch rate (top) and etch yield (bottom) as a function of ICP source power in pure SF_6, NF_3, PF_5, or BF_3 discharges (35mTorr, 5W rf chuck power).

Figure 3. OES spectra from BF_3 (top) and PF_5 (bottom) discharges during etching of Si.

Figure 4. OES spectra from NF_3 (top) and SF_6 (bottom) discharges during etching of Si.

Figure 5. SEM micrographs of Si surfaces after etching in SF_6 (top left), NF_3 (top right), PF_5 (bottom left), and BF_3 (bottom right).

Figure 6. AFM scans of Si surfaces before and after etching in SF_6, NF_3, PF_5, and BF_3.

Figure 7. RSM roughness of Si surfaces after etching in SF_6, NF_3, PF_5, and BF_3.

Figure 8 AES surface scans of Si before (top) and after SF_6 (center) or NF_3 (bottom) etching.

Figure 9. Si etch rate as a function of a) Pressure, b) rf power, and c) ICP power in NF_3 discharges.

Figure 10. AFM scans of Si surfaces before (top) and after (center and bottom) NF_3 etching without (center) or with (bottom) rf biasing of the chuck position.

Table 1. Average bond energies for feedstock gases.

Gas	Avg. Bond Energy (kcal/mol)	Reference
BF_3	154	19
PF_5	126	20
SF_6	78.3	21
NF_3	66.4	22

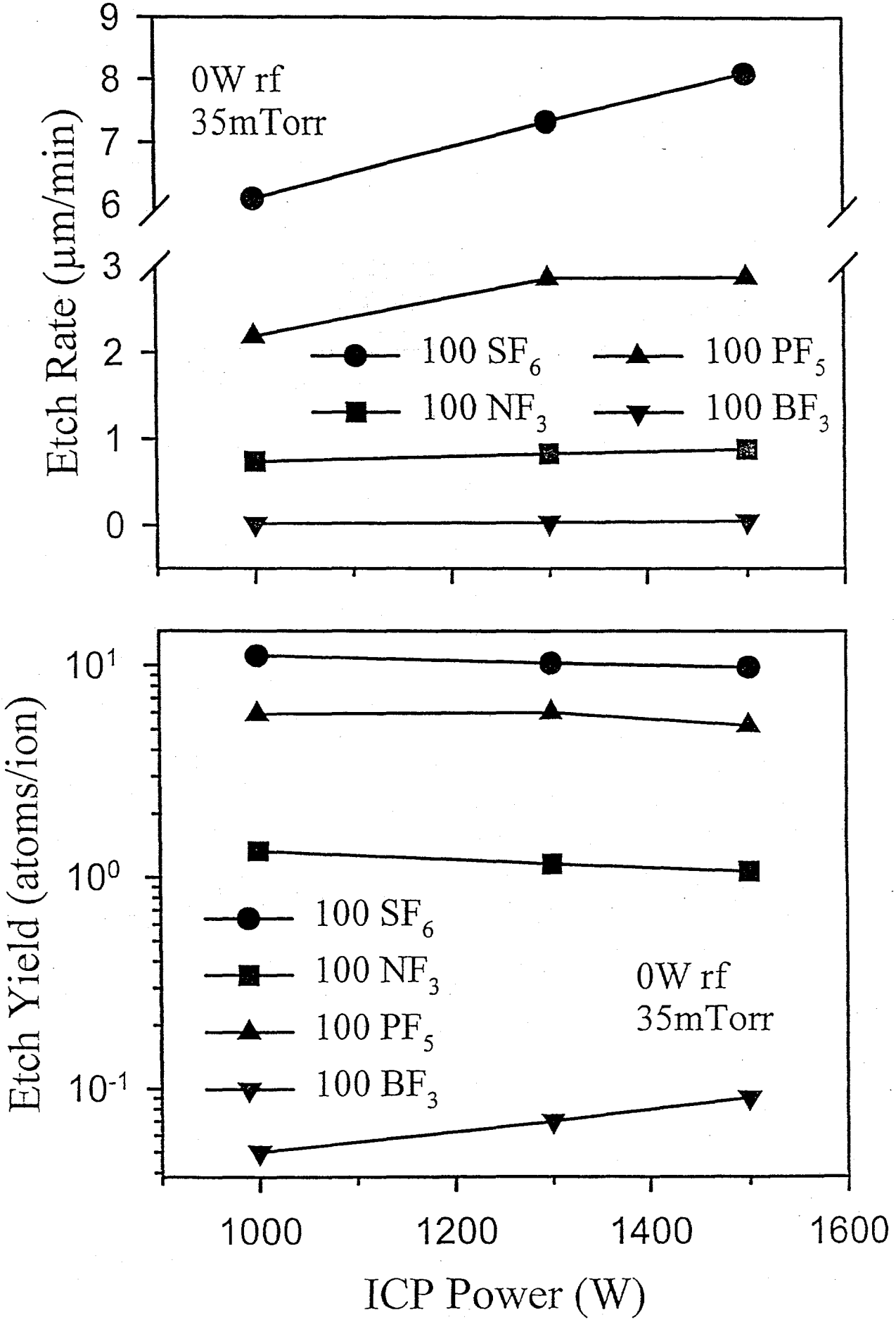
9
8
7
6
3
2
1
0
0W rf
35mTorr
Etch Rate (μm/min)
100 SF6
100 PF5
100 NF3
100 BF3
10^1
10^0
10^-1
Etch Yield (atoms/ion)
100 SF6
100 NF3
100 PF5
100 BF3
0W rf
35mTorr
1000
1200
1400
1600
ICP Power (W)

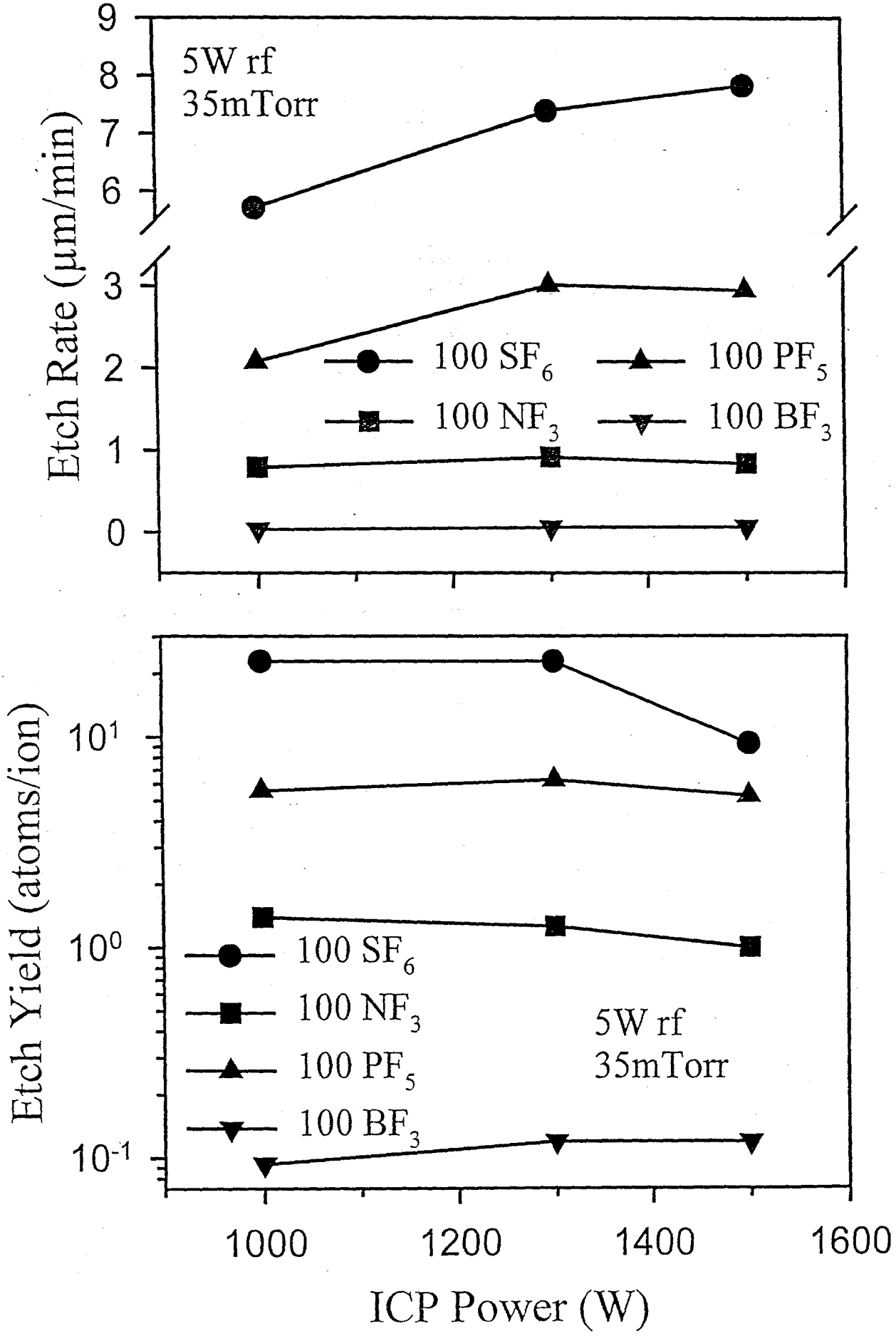
5W rf
35mTorr
Etch Rate (μm/min)
9
8
7
6
3
2
1
0
100 SF6
100 PF5
100 NF3
100 BF3
Etch Yield (atoms/ion)
10^1
10^0
10^-1
100 SF6
100 NF3
100 PF5
100 BF3
5W rf
35mTorr
1000
1200
1400
1600
ICP Power (W)

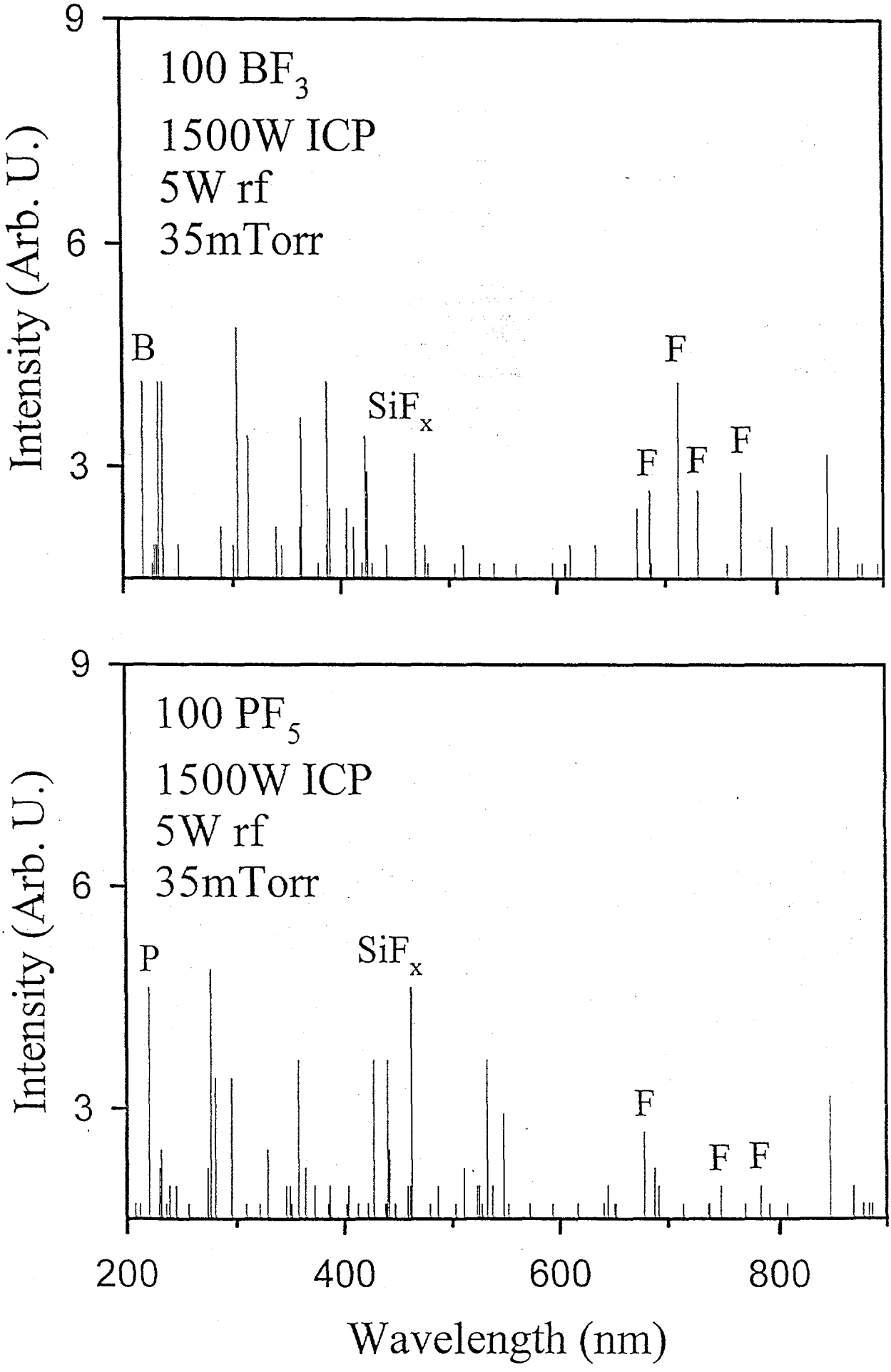
100 BF_3
1500W ICP
5W rf
35mTorr
B
SiF_x
F
F
F
F
Intensity (Arb. U.)
9
6
3
100 PF_5
1500W ICP
5W rf
35mTorr
P
SiF_x
F
F
F
Intensity (Arb. U.)
9
6
3
200
400
600
800
Wavelength (nm)

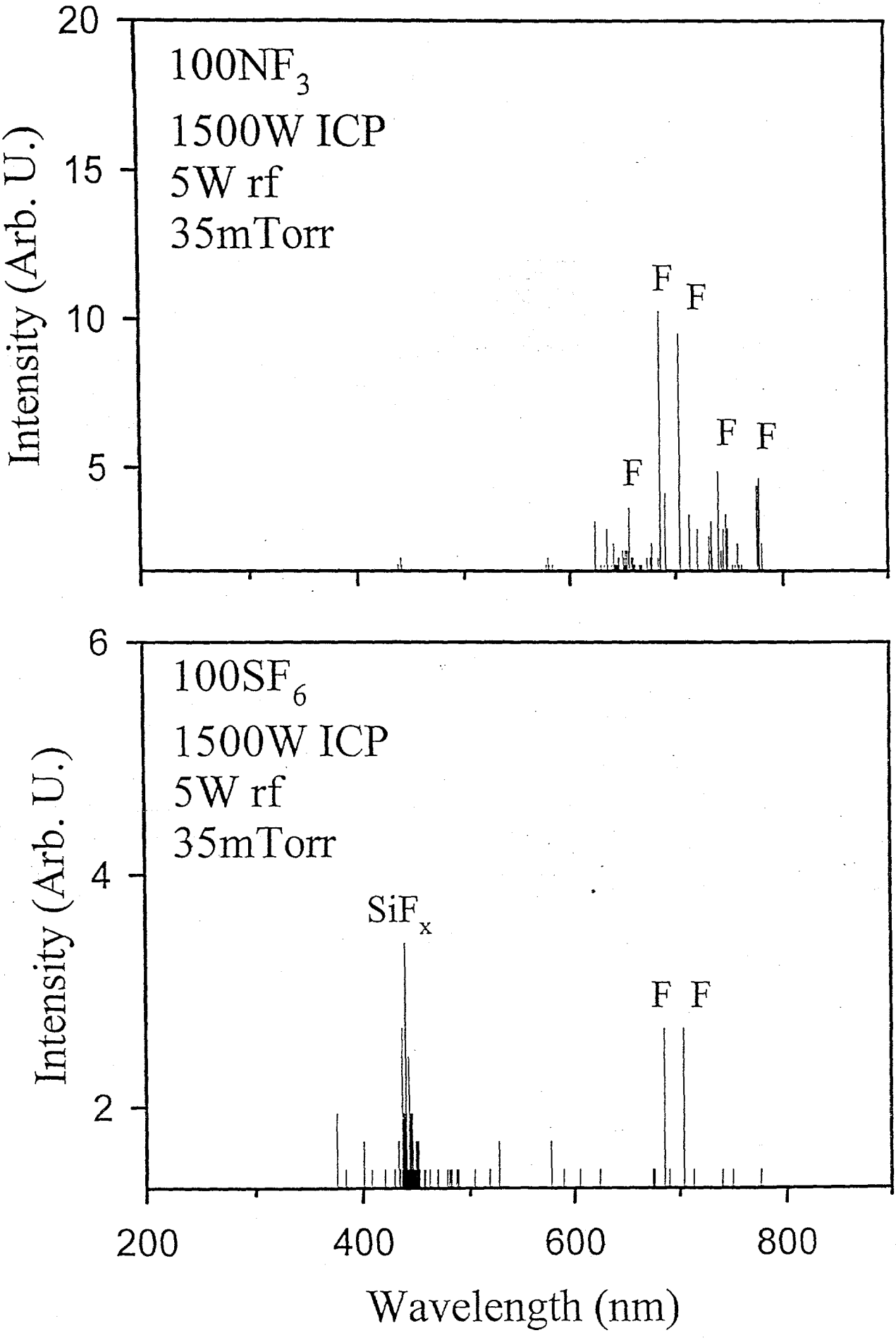
100NF3
1500W ICP
5W rf
35mTorr
Intensity (Arb. U.)
20
15
10
5
F
F
F
F
F
100SF6
1500W ICP
5W rf
35mTorr
Intensity (Arb. U.)
6
4
2
SiFx
F
F
200
400
600
800
Wavelength (nm)

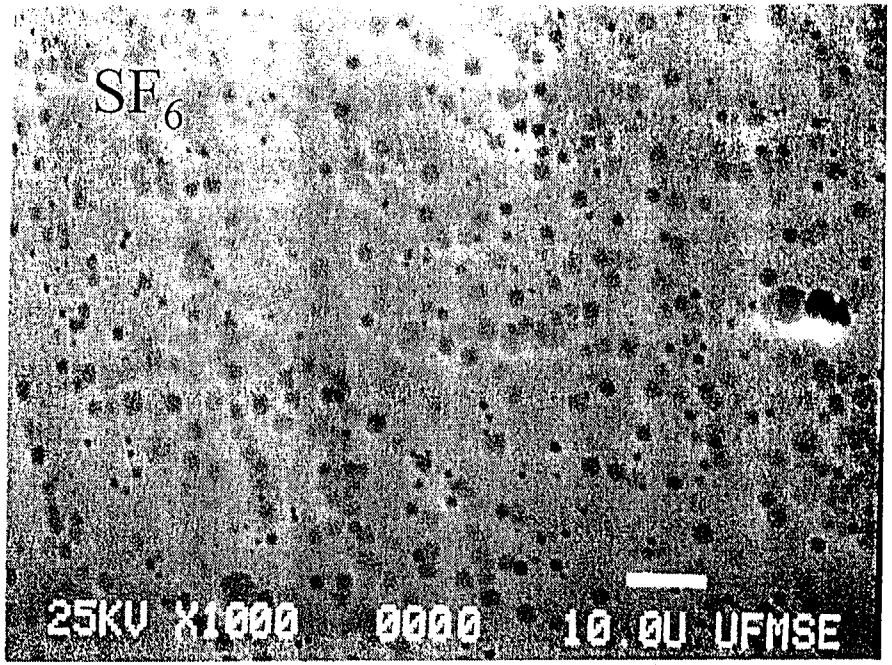
SF_6
25KV X1000 0000 10.0U UFMSE

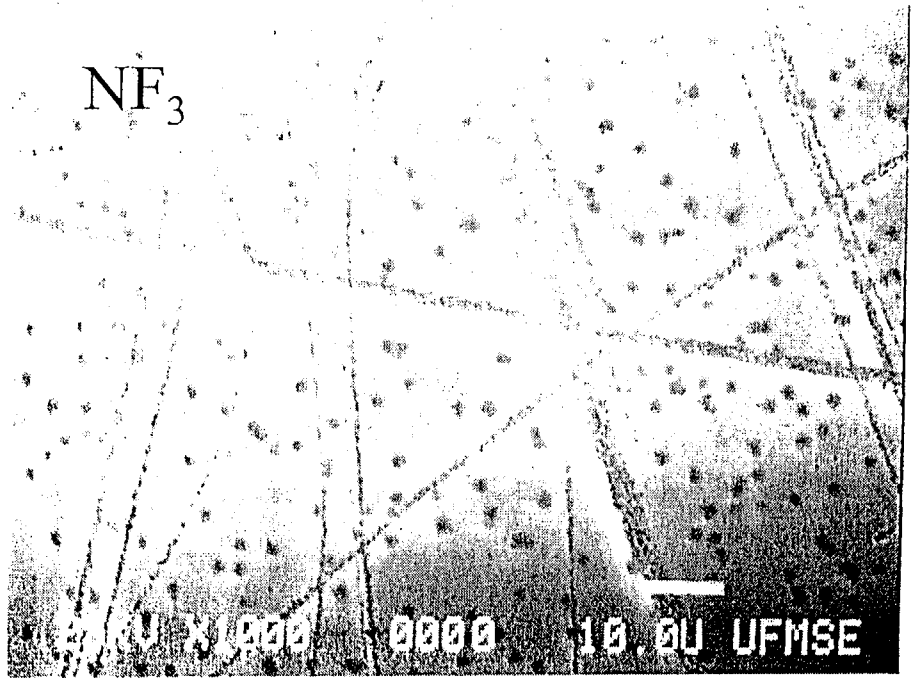
NF_3
10.0U UFMSE

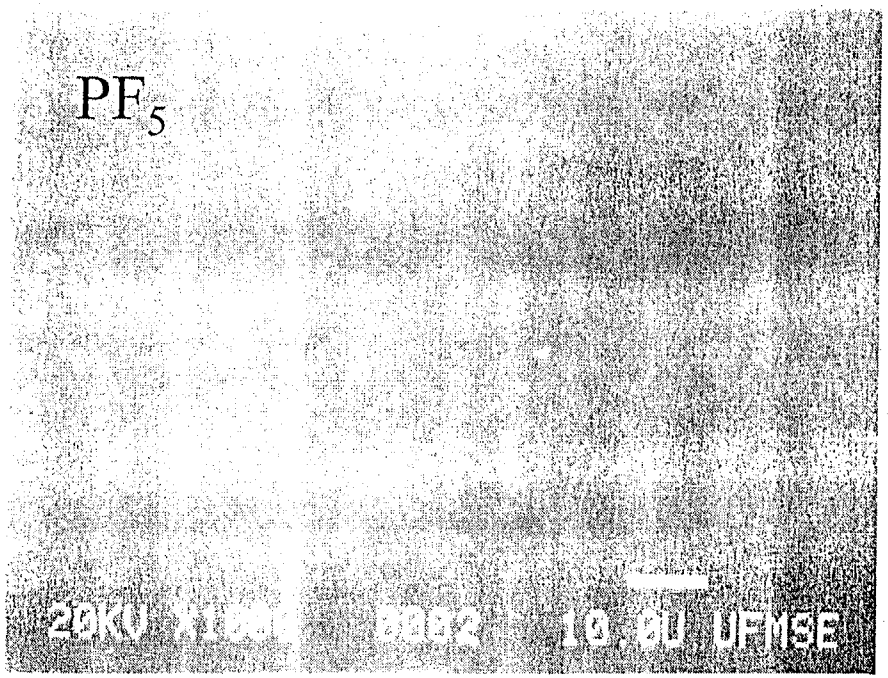
PF_5
10.0U UFMSE

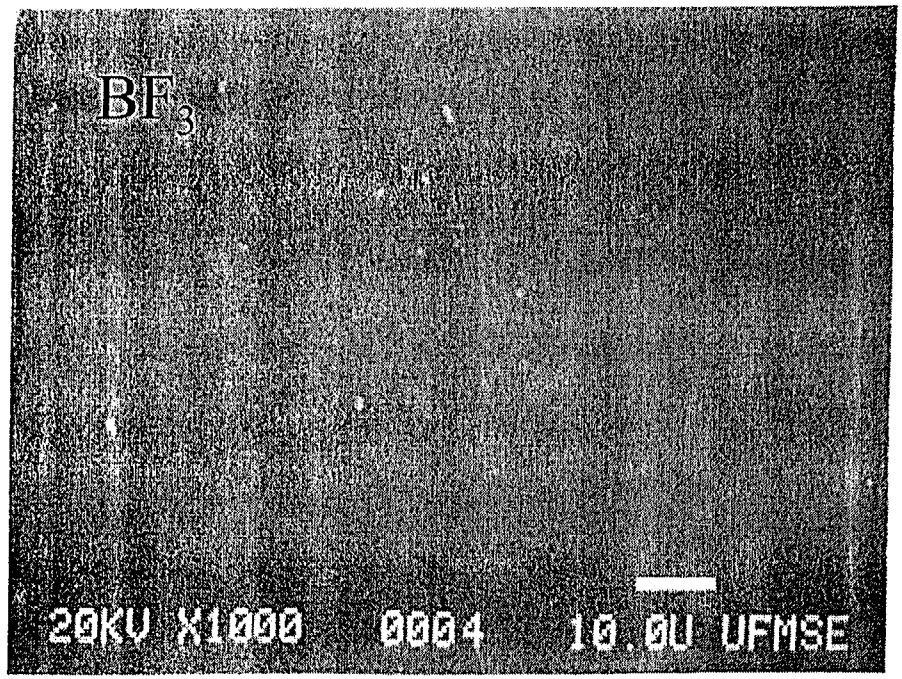
BF_3
20KV X1000 0004 10.0U UFMSE

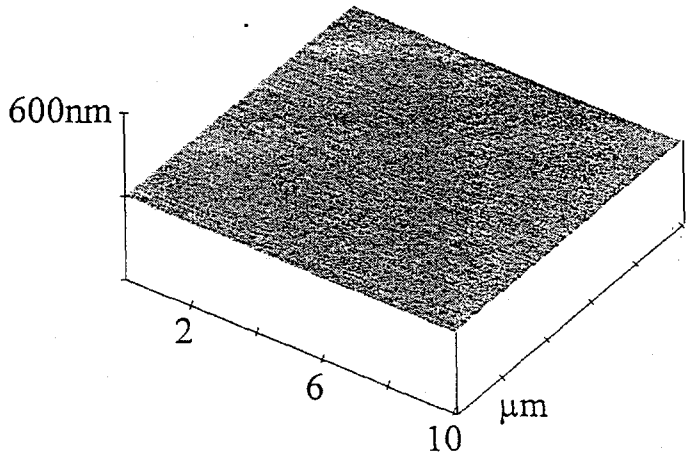

Silicon Control
RMS Roughness = 1.1nm

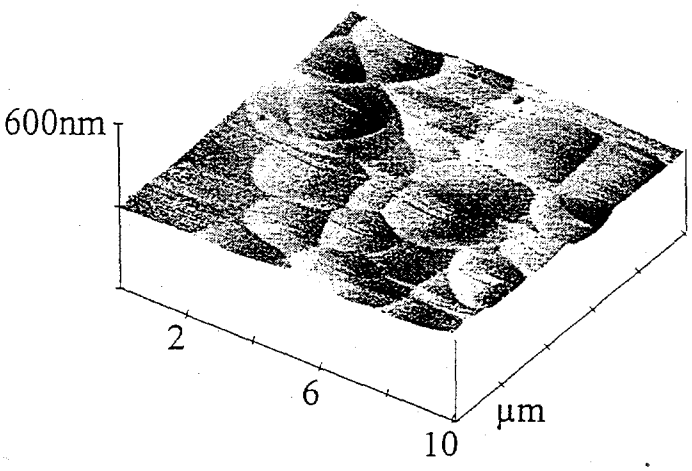

$100SF_6$, 1500W ICP, 0W rf, 35mTorr, 2min.
RMS Roughness = 23.2nm

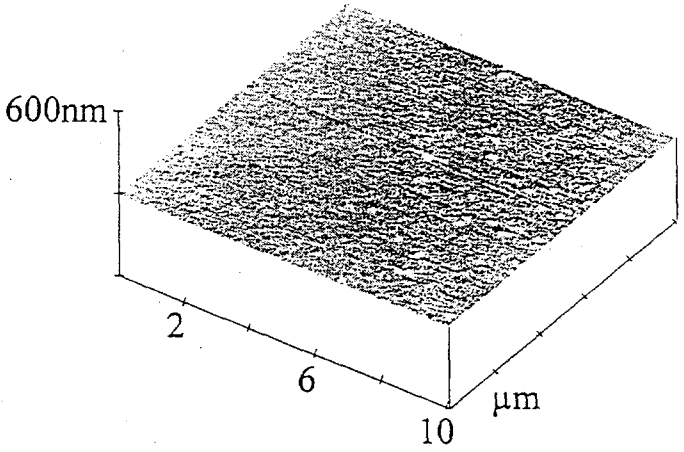

$100PF_5$, 1500W ICP, 0W rf, 35mTorr, 2min.
RMS Roughness = 1.41nm

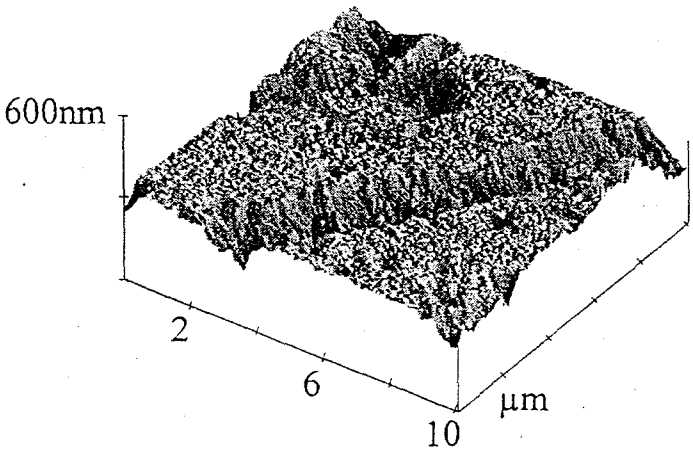

$100NF_3$, 1500W ICP, 0W rf, 35mTorr, 2min.
RMS Roughness = 67.1nm

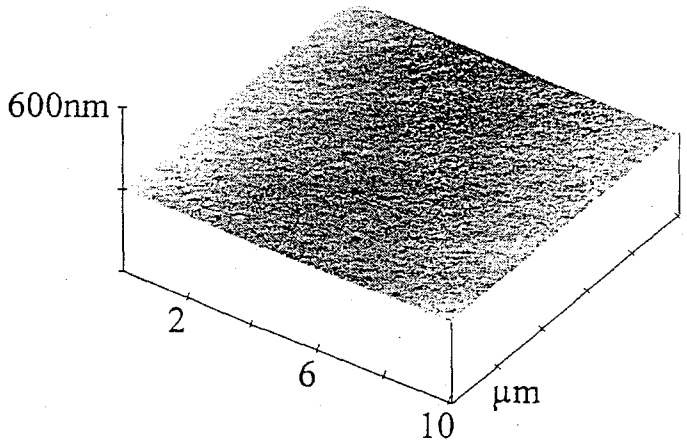

$100BF_3$, 1500W ICP, 0W rf, 35mTorr, 2min.
RMS Roughness = 1.17nm

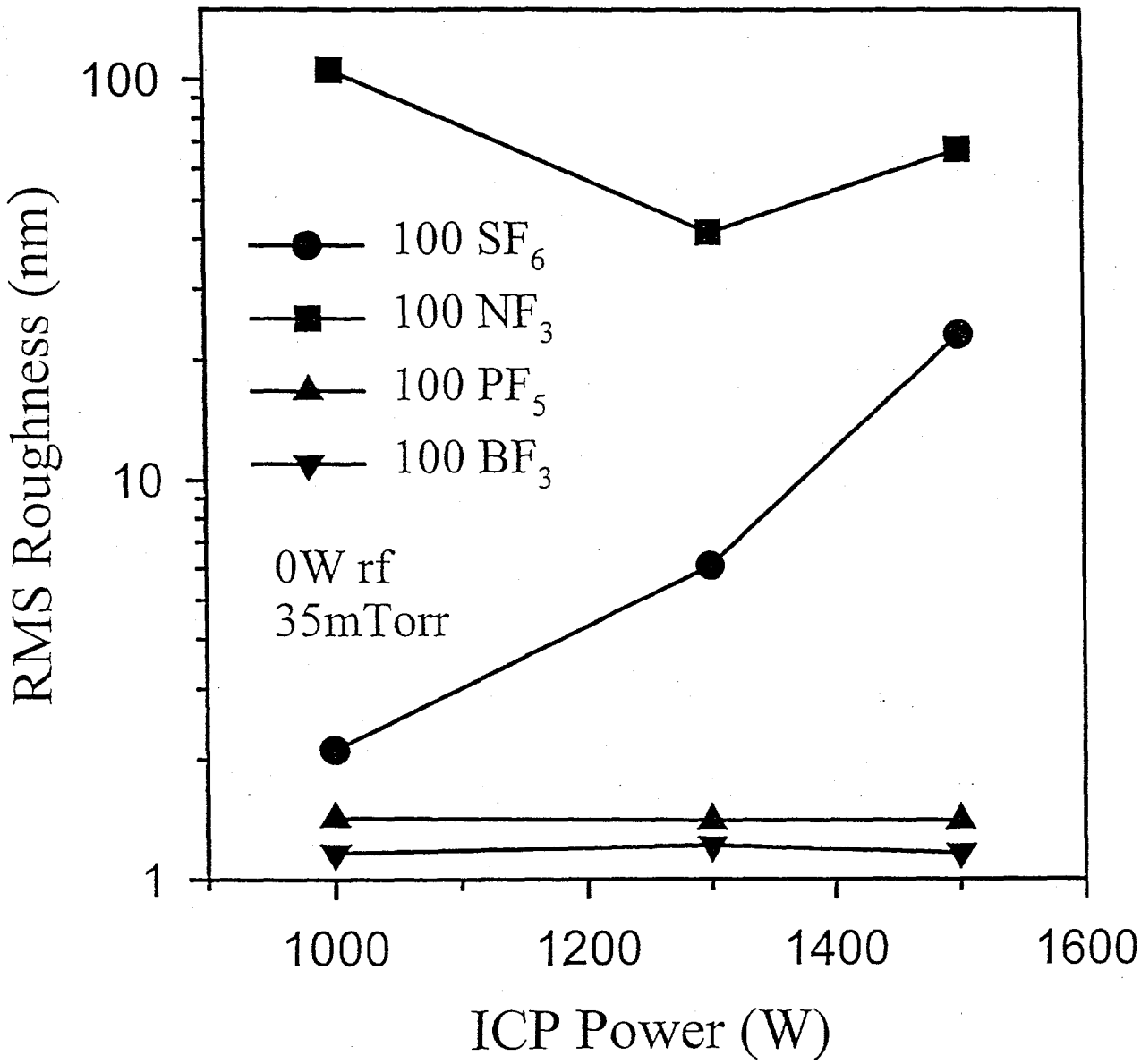
RMS Roughness (nm)
100
10
1
100 SF6
100 NF3
100 PF5
100 BF3
0W rf
35mTorr
1000
1200
1400
1600
ICP Power (W)

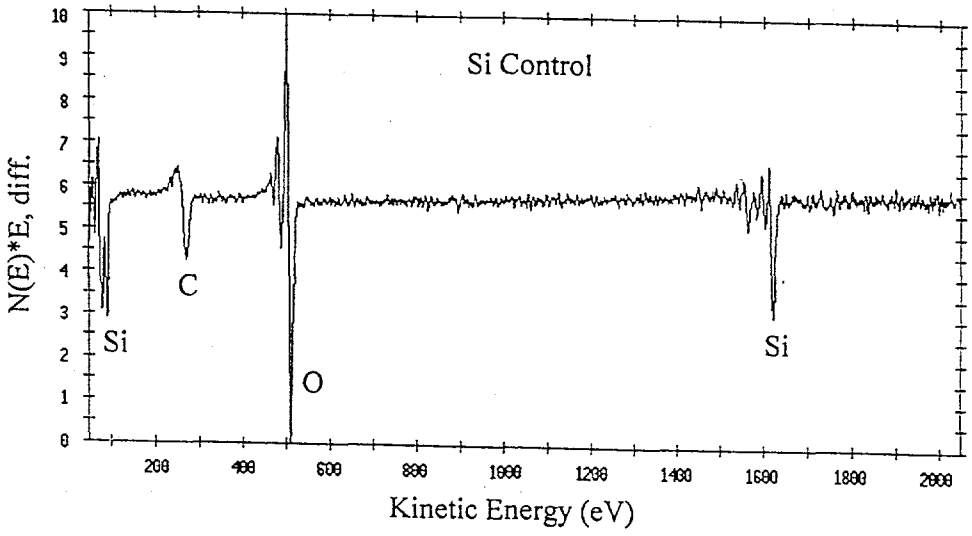
Si Control
N(E)*E, diff.
Si
C
O
Si
Kinetic Energy (eV)

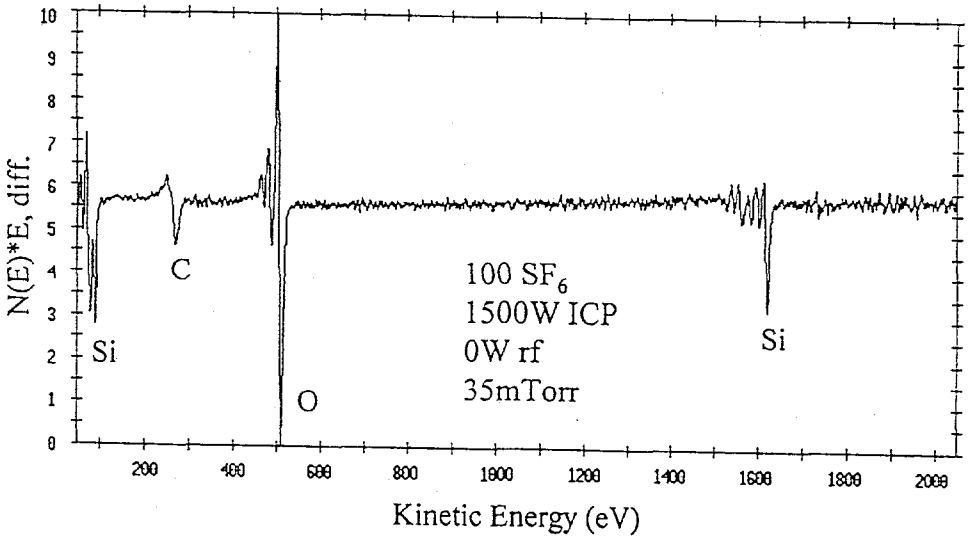
100 SF6
1500W ICP
0W rf
35mTorr
N(E)*E, diff.
Si
C
O
Si
Kinetic Energy (eV)

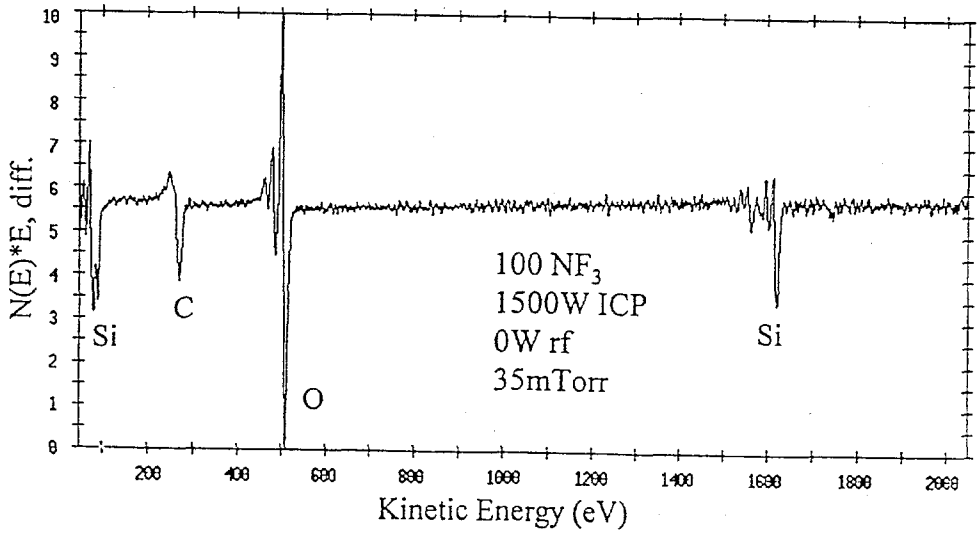
100 NF3
1500W ICP
0W rf
35mTorr
N(E)*E, diff.
Si
C
O
Si
Kinetic Energy (eV)

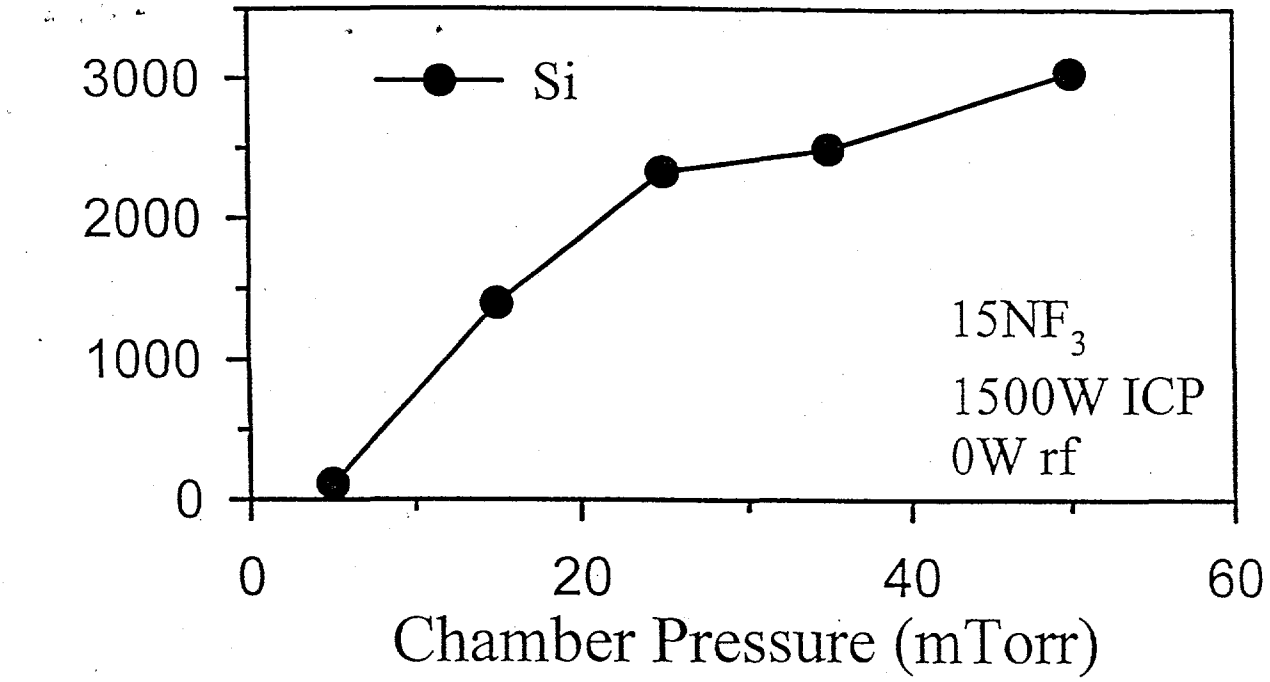
Si
3000
2000
1000
0
0
20
40
60
15NF3
1500W ICP
0W rf
Chamber Pressure (mTorr)

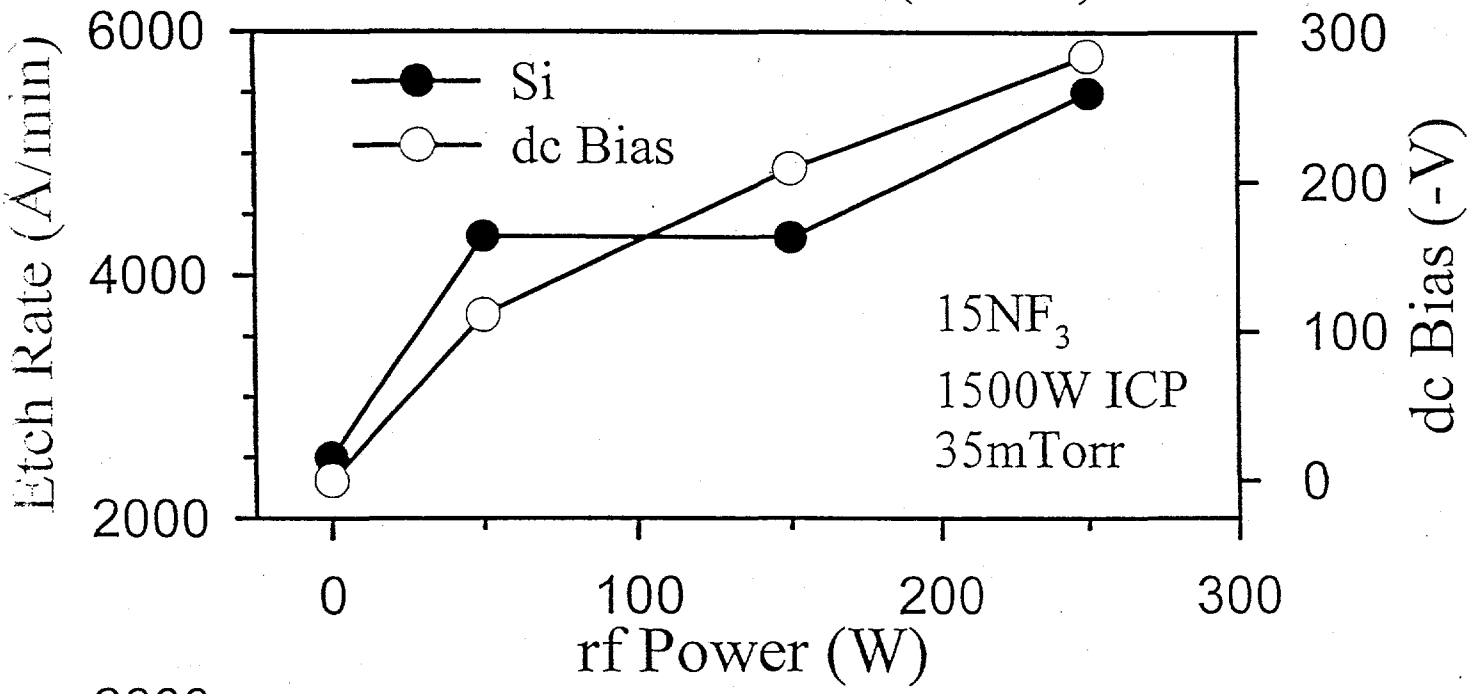
Si
dc Bias
6000
4000
2000
300
200
100
0
0
100
200
300
15NF3
1500W ICP
35mTorr
Etch Rate (Å/min)
dc Bias (-V)
rf Power (W)

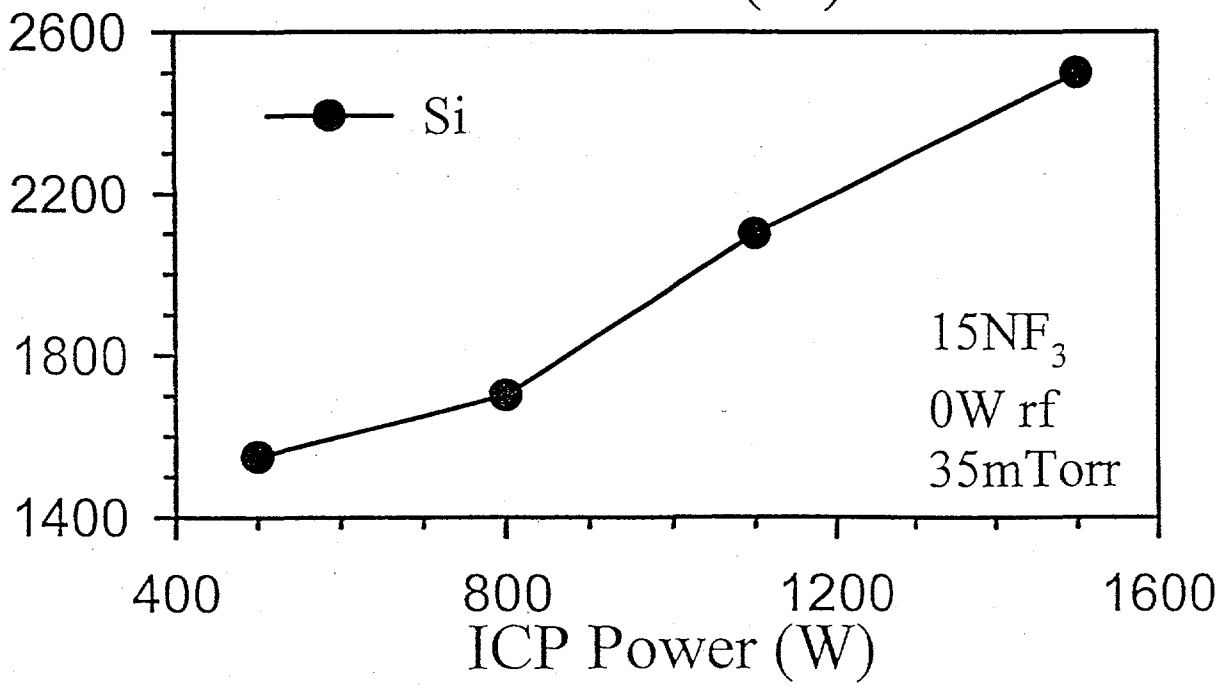
Si
2600
2200
1800
1400
400
800
1200
1600
15NF3
0W rf
35mTorr
ICP Power (W)

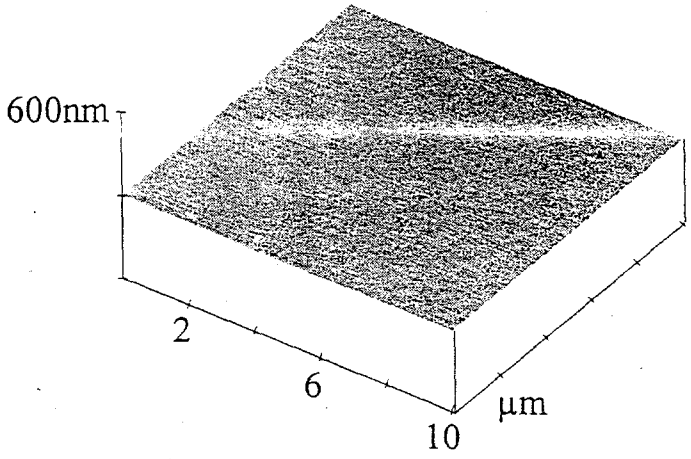

Silicon Control
RMS Roughness = 1.1nm

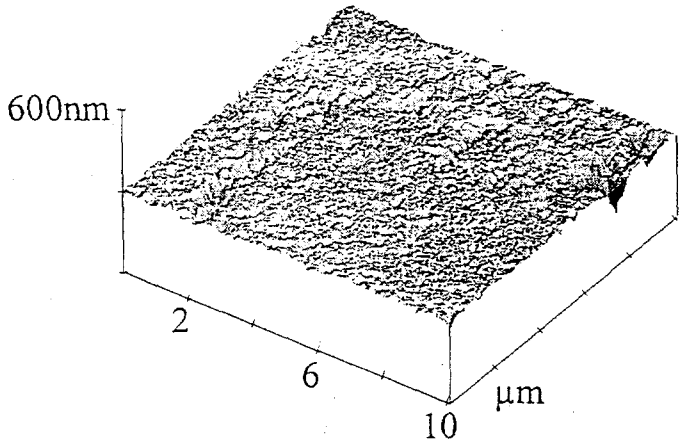

$15NF_3$, 1500W ICP, 0W rf, 35mTorr, 2min.
RMS Roughness = 24.3nm

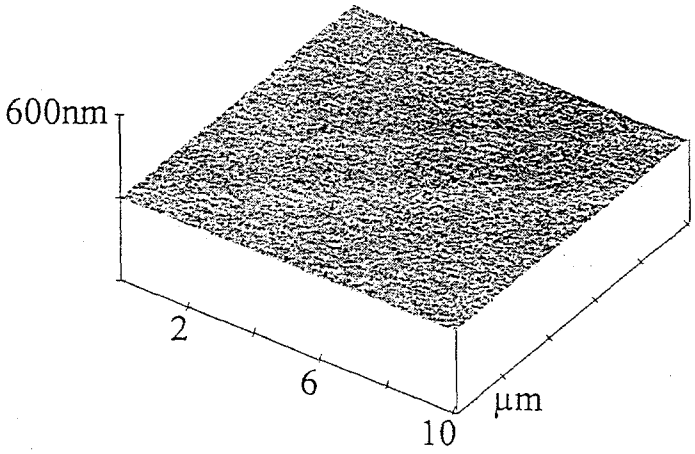

$15NF_3$, 1500W ICP, 250W rf, 35mTorr, 2min.
RMS Roughness = 1.3nm